2

Ion channels and the Hodgkin–Huxley model

From a biophysical point of view, action potentials are the result of currents that pass through ion channels in the cell membrane. In an extensive series of experiments on the giant axon of the squid, Hodgkin and Huxley succeeded in measuring these currents and described their dynamics in terms of differential equations. Their paper published in 1952, which presents beautiful experiments combined with an elegant mathematical theory (Hodgkin and Huxley, 1952), was rapidly recognized as groundbreaking work and eventually led to the Nobel Prize for Hodgkin and Huxley in 1963. In this chapter, the Hodgkin–Huxley model is reviewed and its behavior illustrated by several examples.

The Hodgkin–Huxley model in its original form describes only three types of ion channel. However, as we shall see in Section 2.3 it can be extended to include many other ion channel types. The Hodgkin–Huxley equations are the basis for detailed neuron models which account for different types of synapse, and the spatial geometry of an individual neuron. Synaptic dynamics and the spatial structure of dendrites are the topics of Chapter 3. The Hodgkin–Huxley model is also the starting point for the derivation of simplified neuron models in Chapter 4 and will serve as a reference throughout the discussion of generalized integrate-and-fire models in Part II of the book.

Before we can turn to the Hodgkin–Huxley equations, we need to give some additional information on the equilibrium potential of ion channels.

2.1 Equilibrium potential

Neurons, just as other cells, are enclosed by a membrane which separates the interior of the cell from the extracellular space. Inside the cell the concentration of ions is different from that in the surrounding liquid. The difference in concentration generates an electrical potential which plays an important role in neuronal dynamics. In this section, we provide some background information and give an intuitive explanation of the equilibrium potential.

https://doi.org/10.1017/CBO9781107447615.003 Published online by Cambridge University Press

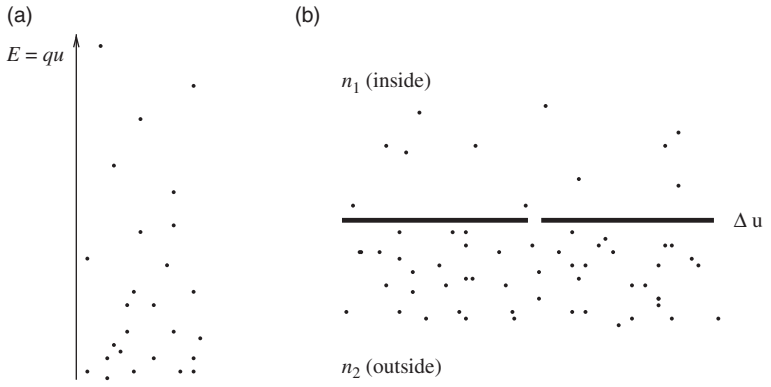

Fig. 2.1 (a) At thermal equilibrium, positive ions in an electric field will be distributed so that fewer ions are in a state of high energy and more at low energy. Thus a voltage difference generates a gradient in concentration. (b) Similarly, a difference in ion concentration generates an electrical potential. The concentration n_2 inside the neuron is different from the concentration n_1 of the surround. The resulting potential is called the Nernst potential. The solid line indicates the cell membrane. Ions can pass through the gap.

2.1.1 Nernst potential

From the theory of thermodynamics, it is known that the probability of a molecule taking a state of energy E is proportional to the Boltzmann factor, $p(E) \propto \exp(-E/kT)$, where k is the Boltzmann constant and T the temperature. Let us consider positive ions with charge q in a static electrical field. Their energy at location x is $E(x) = q\,u(x)$ where $u(x)$ is the potential at x. The probability of finding an ion in the region around x is therefore proportional to $\exp[-q\,u(x)/kT]$. Since the number of ions is huge, we may interpret the probability as an ion density. For ions with positive charge $q > 0$, the ion density is therefore higher in regions with low potential u. Let us write $n(x)$ for the ion density at point x. The relation between the density at point x_1 and point x_2 is

$$\frac{n(x_1)}{n(x_2)} = \exp\left[-\frac{q\,u(x_1) - q\,u(x_2)}{kT}\right]. \tag{2.1}$$

A difference in the electrical potential $\Delta u = u(x_1) - u(x_2)$ generates therefore a difference in ion density; see Fig. 2.1.

Since this is a statement about an equilibrium state, the reverse must also be true. A difference in ion density generates a difference Δu in the electrical potential. We consider two regions of ions with concentration n_1 and n_2, respectively; see Fig. 2.1b. Solving (2.1) for Δu we find that, at equilibrium, the concentration difference generates a voltage

$$\Delta u = \frac{kT}{q} \ln \frac{n_2}{n_1} \tag{2.2}$$

which is called the Nernst potential (Hille, 2001).

https://doi.org/10.1017/CBO9781107447615.003 Published online by Cambridge University Press

2.1.2 Reversal potential

The cell membrane consists of a thin bilayer of lipids and is a nearly perfect electrical insulator. Embedded in the cell membrane are, however, specific proteins which act as ion gates. A first type of gate is the ion pumps, a second one is ion channels. Ion pumps actively transport ions from one side to the other. As a result, ion concentrations in the intracellular liquid differ from those of the surround. For example, the sodium concentration inside a mammalian neuron ($\approx 10\,\text{mM}$) is lower than that in the extracellular liquid ($\approx 145\,\text{mM}$). On the other hand, the potassium concentration inside is higher ($\approx 140\,\text{mM}$) than in the surround ($\approx 5\,\text{mM}$) (Purves *et al.*, 2008). For the giant axon of the squid which was studied by Hodgkin and Huxley the numbers are slightly different, but the basic idea is the same: there is more sodium outside the cell than inside, while the reverse is true for potassium.

Let us focus for the moment on sodium ions. At equilibrium the difference in concentration causes a Nernst potential E_{Na} of about +67 mV. That is, at equilibrium the interior of the cell has a positive potential with respect to the surround. The interior of the cell and the surrounding liquid are in contact through ion channels where Na^+ ions can pass from one side of the membrane to the other. If the voltage difference Δu is smaller than the value of the Nernst potential E_{Na}, more Na^+ ions flow into the cell so as to decrease the concentration difference. If the voltage is larger than the Nernst potential ions would flow out the cell. Thus the direction of the current is reversed when the voltage Δu passes E_{Na}. For this reason, E_{Na} is called the reversal potential.

Example: Reversal potential for potassium

As mentioned above, the ion concentration of potassium is higher inside the cell ($\approx 140\,\text{mM}$) than in the extracellular liquid ($\approx 5\,\text{mM}$). Potassium ions have a single positive charge $q = 1.6 \times 10^{-19}\,\text{C}$. Application of the Nernst formula, (2.2), with the Boltzmann constant $k = 1.4 \times 10^{-23}\,\text{J/K}$ yields $E_{\text{K}} \approx -83\,\text{mV}$ at room temperature. The reversal potential for K^+ ions is therefore negative.

Example: Resting potential

So far we have considered the presence of either sodium or potassium. In real cells, these and other ion types are simultaneously present and contribute to the voltage across the membrane. It is found experimentally that the resting potential of the membrane is about $u_{\text{rest}} \approx 65\,\text{mV}$. Since $E_{\text{K}} < u_{\text{rest}} < E_{\text{Na}}$, potassium ions, at the resting potential, flow out of the cell while sodium ions flow into the cell. In the stationary state, the active ion pumps balance this flow and transport just as many ions back as pass through

https://doi.org/10.1017/CBO9781107447615.003 Published online by Cambridge University Press

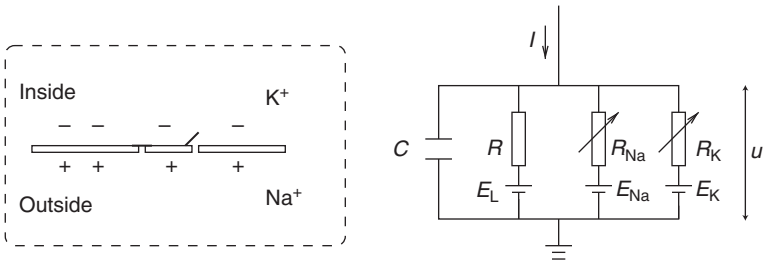

Fig. 2.2 Schematic diagram for the Hodgkin–Huxley model.

the channels. The value of u_{rest} is determined by the dynamic equilibrium between the ion flow through the channels (permeability of the membrane) and active ion transport (efficiency of the ion pump in maintaining the concentration difference).

2.2 Hodgkin–Huxley model

Hodgkin and Huxley (1952) performed experiments on the giant axon of the squid and found three different types of ion current, namely, sodium, potassium, and a leak current that consists mainly of Cl^- ions. Specific voltage-dependent ion channels, one for sodium and another one for potassium, control the flow of those ions through the cell membrane. The leak current takes care of other channel types which are not described explicitly.

2.2.1 Definition of the model

The Hodgkin–Huxley model can be understood with the help of Fig. 2.2. The semipermeable cell membrane separates the interior of the cell from the extracellular liquid and acts as a capacitor. If an input current $I(t)$ is injected into the cell, it may add further charge on the capacitor, or leak through the channels in the cell membrane. Each channel type is represented in Fig. 2.2 by a resistor. The unspecific channel has a leak resistance R, the sodium channel a resistance R_{Na} and the potassium channel a resistance R_{K}. The diagonal arrow across the diagram of the resistor indicates that the value of the resistance is not fixed, but changes depending on whether the ion channel is open or closed. Because of active ion transport through the cell membrane, the ion concentration inside the cell is different from that in the extracellular liquid. The Nernst potential generated by the difference in ion concentration is represented by a battery in Fig. 2.2. Since the Nernst potential is different for each ion type, there are separate batteries for sodium, potassium, and the unspecific third channel, with battery voltages $E_{\text{Na}}, E_{\text{K}}$ and E_{L}, respectively.

Let us now translate the above schema of an electrical circuit into mathematical equations. The conservation of electric charge on a piece of membrane implies that the applied current $I(t)$ may be split into a capacitive current I_C which charges the capacitor C and

https://doi.org/10.1017/CBO9781107447615.003 Published online by Cambridge University Press

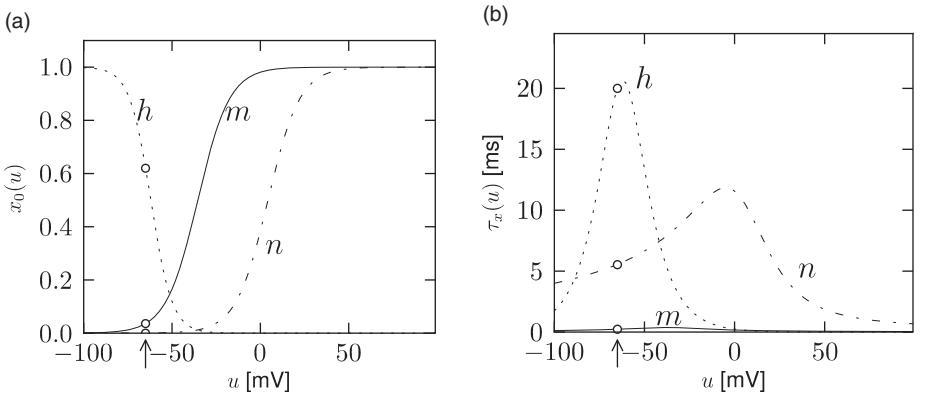

Fig. 2.3 The Hodgkin–Huxley model. (a) The equilibrium functions for the three variables m,n,h in the Hodgkin–Huxley model. (b) The voltage-dependent time constant. The resting potential is at $u = -65\,\mathrm{mV}$ (arrow) and parameters are those given in Table 2.1.

further components I_k which pass through the ion channels. Thus

$$I(t) = I_C(t) + \sum_k I_k(t), \tag{2.3}$$

where the sum runs over all ion channels. In the standard Hodgkin–Huxley model there are only three types of channel: a sodium channel with index Na, a potassium channel with index K and an unspecific leakage channel with resistance R; see Fig. 2.2. From the definition of a capacity $C = q/u$ where q is a charge and u the voltage across the capacitor, we find the charging current $I_C = C\,\mathrm{d}u/\mathrm{d}t$. Hence from (2.3)

$$C\frac{\mathrm{d}u}{\mathrm{d}t} = -\sum_k I_k(t) + I(t)\,. \tag{2.4}$$

In biological terms, u is the voltage across the membrane and $\sum_k I_k$ is the sum of the ionic currents which pass through the cell membrane.

As mentioned above, the Hodgkin–Huxley model describes three types of channel. All channels may be characterized by their resistance or, equivalently, by their conductance. The leakage channel is described by a voltage-independent conductance $g_\mathrm{L} = 1/R$. Since u is the total voltage across the cell membrane and E_L the voltage of the battery, the voltage at the leak resistor in Fig. 2.2 is $u - E_\mathrm{L}$. Using Ohm's law, we get a leak current $I_\mathrm{L} = g_\mathrm{L}\,(u - E_\mathrm{L})$.

The mathematics of the other ion channels is analogous except that their conductance is voltage- and time-dependent. If all channels are open, they transmit currents with a maximum conductance g_Na or g_K, respectively. Normally, however, some of the channels are blocked. The breakthrough of Hodgkin and Huxley was that they succeeded in measuring how the effective resistance of a channel changes as a function of time and voltage. Moreover, they proposed a mathematical description of their observations. Specifically, they introduced additional "gating" variables m,n and h to model the probability that a

https://doi.org/10.1017/CBO9781107447615.003 Published online by Cambridge University Press

x	E_x [mV]	g_x [mS/cm^2]
Na	55	40
K	−77	35
L	−65	0.3

x	$\alpha_x(u/\text{mV})$ [ms^{-1}]	$\beta_x(u/\text{mV})$ [ms^{-1}]
n	$0.02(u-25)/[1-e^{-(u-25)/9}]$	$-0.002(u-25)/[1-e^{(u-25)/9}]$
m	$0.182(u+35)/[1-e^{-(u+35)/9}]$	$-0.124(u+35)/[1-e^{(u+35)/9}]$
h	$1/[1+e^{-(u+62)/6}]$	$4e^{(u+90)/12}/[1+e^{-(u+62)/6}]$

Table 2.1 *Parameters for the Hodgkin–Huxley equations fitted on pyramidal neurons of the cortex. The parameters for n and m were fitted by Zach Mainen (Mainen et al., 1995) on experiments reported by Huguenard et al. (1988) and the parameters for h by Richard Naud on the experiments reported in Hamill et al. (1991). Voltage is measured in mV and the membrane capacity is* $C = 1\,\mu F/cm^2$.

channel is open at a given moment in time. The combined action of m and h controls the Na^+ channels while the K^+ gates are controlled by n. For example, the effective conductance of sodium channels is modeled as $1/R_{\text{Na}} = g_{\text{Na}}\, m^3\, h$, where m describes the activation (opening) of the channel and h its inactivation (blocking). The conductance of potassium is $1/R_{\text{K}} = g_{\text{K}}\, n^4$, where n describes the activation of the channel.

In summary, Hodgkin and Huxley formulated the three ion currents on the right-hand-side of (2.4) as

$$\sum_k I_k = g_{\text{Na}}\, m^3 h\,(u - E_{\text{Na}}) + g_{\text{K}}\, n^4\,(u - E_{\text{K}}) + g_{\text{L}}\,(u - E_{\text{L}}). \tag{2.5}$$

The parameters E_{Na}, E_{K}, and E_{L} are the reversal potentials.

The three gating variables m, n, and h evolve according to differential equations of the form

$$\dot{x} = -\frac{1}{\tau_x(u)}[x - x_0(u)], \tag{2.6}$$

with $\dot{x} = \mathrm{d}x/\mathrm{d}t$, and where x stands for m, n, or h. The interpretation of (2.6) is simple: for a fixed voltage u, the variable x approaches the target value $x_0(u)$ with a time constant $\tau_x(u)$. The voltage dependence of the time constant and asymptotic value is illustrated in Fig. 2.3. The form of the functions plotted in Fig. 2.3, as well as the maximum conductances and reversal potentials in (2.5), were deduced by Hodgkin and Huxley from empirical measurements.

Example: Voltage step

Experimenters can hold the voltage across the cell membrane at a desired value by injecting an appropriate current into the cell. Suppose that the experimenter keeps the

https://doi.org/10.1017/CBO9781107447615.003 Published online by Cambridge University Press

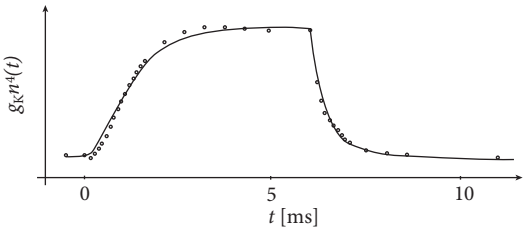

Fig. 2.4 Original data and fit of Hodgkin and Huxley (1952). The measured time course of the potassium conductance (circles) after application of a voltage step of 25 mV and after return to resting potential. The fit (solid line) is based on Eq. (2.8). Adapted from Hodgkin and Huxley (1952).

cell at resting potential $u_0 = -65\,\text{mV}$ for $t < t_0$ and switches the voltage at t_0 to a new value u_1. Integration of the differential equation (2.6) gives, for $t > t_0$, the dynamics

$$m(t) = m_0(u_1) + [m_0(u_0) - m_0(u_1)] \exp\left[\frac{-(t-t_0)}{\tau_m(u_1)}\right],$$
$$h(t) = h_0(u_1) + [h_0(u_0) - h_0(u_1)] \exp\left[\frac{-(t-t_0)}{\tau_h(u_1)}\right], \tag{2.7}$$

so that, based on the model with given functions for $m_0(u)$, $h_0(u)$, $\tau_m(u)$, $\tau_h(u)$, we can predict the sodium current $I_{\text{Na}}(t) = g_{\text{Na}}\,[m(t)^3]\,h(t)\,(u_1 - E_{\text{Na}})$ for $t > t_0$ generated by the voltage step at $t = t_0$.

Similarly, the potassium current caused by a voltage step is $I_{\text{K}}(t) = g_{\text{K}}\,[n(t)^4]\,(u_1 - E_{\text{K}})$ with

$$n(t) = n_0(u_1) + [n_0(u_0) - n_0(u_1)] \exp\left[\frac{-(t-t_0)}{\tau_n(u_1)}\right]. \tag{2.8}$$

Hodgkin and Huxley used Eqs. (2.7) and (2.8) to work the other way round. After blocking the sodium channel with appropriate pharmacological agents, they applied a voltage step and measured the time course of the potassium current. Dividing the recorded current through the driving potential $(u_1 - E_{\text{K}})$ yields the time-dependent conductance $g_{\text{K}}\,[n(t)^4]$; see Fig. 2.4. Using (2.8), Hodgkin and Huxley deduced the value of $n_0(u_1)$ and $\tau_n(u_1)$ as well as the exponent of 4 in $n^4(t)$ for potassium. Repeating the experiments for different values u_1 gives the experimental curves for $n_0(u)$ and $\tau_n(u)$.

Example: Activation and de-inactivation

The variable m is called an activation variable. To understand this terminology, we note from Fig. 2.3 that the value of $m_0(u)$ at the neuronal resting potential of $u = -65\,\text{mV}$ is close to zero. Therefore, at rest, the sodium current $I_{\text{Na}} = g_{\text{Na}}\,m^3 h\,(u - E_{\text{Na}})$ through the channel vanishes. In other words, the sodium channel is closed.

When the membrane potential increases significantly above the resting potential, the gating variable m increases to its new value $m_0(u)$. As long as h does not change, the

https://doi.org/10.1017/CBO9781107447615.003 Published online by Cambridge University Press

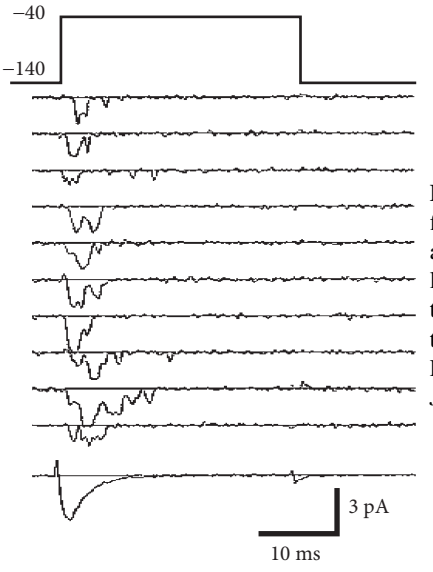

Fig. 2.5 Stochastic channel activation. The current flowing through a small patch of membrane after application of a voltage step (top row) shows step-like changes and is different in each trial (subsequent traces). Averaging over many trials yields the bottom trace. Adapted from Patlak and Ortiz (1985). ©1985 Rockefeller University Press. Originally published in *Journal of General Physiology*, **86**: 89–104.

sodium current increases and the gate opens. Therefore the variable m "activates" the channel. If, after a return of the voltage to rest, m decays back to zero, it is said to be "de-activating."

The terminology of the "inactivation" variable h is analogous. At rest, h has a large positive value. If the voltage increases to a value above $-40\,\mathrm{mV}$, h approaches a new value $h_0(u)$ which is close to rest. Therefore the channel "inactivates" (blocks) with a time constant that is given by $\tau_h(u)$. If the voltage returns to zero, h increases so that the channel undergoes "de-inactivation." This sounds like tricky vocabulary, but it turns out to be useful to distinguish between a deactivated channel (m close to zero and h close to 1) and an inactivated channel (h close to zero).

2.2.2 Stochastic channel opening

The number of ion channels in a patch of membrane is finite, and individual ion channels open and close stochastically. Thus, when an experimenter records the current flowing through a small patch of membrane, he does not find a smooth and reliable evolution of the measured variable over time but rather a highly fluctuating current, which looks different at each repetition of the experiment (Fig. 2.5).

The Hodgkin–Huxley equations, which describe the opening and closing of ion channels with deterministic equations for the variables m, h, and n, correspond to the current density through a hypothetical, extremely large patch of membrane containing an infinite number of channels or, alternatively, to the current through a small patch of membrane but averaged over many repetitions of the same experiment (Fig. 2.5). The stochastic aspects can be included by adding appropriate noise to the model.

Example: Time constants, transition rates, and channel kinetics

As an alternative to the formulation of channel gating in Eq. (2.6), the activation and inactivation dynamics of each channel type can also be described in terms of voltage-dependent transition rates α and β,

$$\begin{aligned} \dot{m} &= \alpha_m(u)\,(1-m) - \beta_m(u)\,m, \\ \dot{n} &= \alpha_n(u)\,(1-n) - \beta_n(u)\,n, \\ \dot{h} &= \alpha_h(u)\,(1-h) - \beta_h(u)\,h. \end{aligned} \tag{2.9}$$

The two formulations Eqs. (2.6) and (2.9) are equivalent. The asymptotic value $x_0(u)$ and the time constant $\tau_x(u)$ are given by the transformation $x_0(u) = \alpha_x(u)/[\alpha_x(u)+\beta_x(u)]$ and $\tau_x(u) = [\alpha_x(u)+\beta_x(u)]^{-1}$. The various functions α and β, given in Table 2.1, are empirical functions of u that produce the curves in Fig. 2.3.

Equations (2.9) are typical equations used in chemistry to describe the stochastic dynamics of an activation process with rate constants α and β. We may interpret this process as a molecular switch between two states with voltage-dependent transition rates. For example, the activation variable n can be interpreted as the probability of finding a single potassium channel open. Therefore in a patch with K channels, $k \approx (1-n)K$ channels are expected to be closed. We may interpret $\alpha_n(u)\Delta t$ as the probability that in a short time interval Δt one of the momentarily closed channels switches to the open state.

2.2.3 Dynamics

In this section we study the dynamics of the Hodgkin–Huxley model for different types of input. Pulse input, constant input, step current input, and time-dependent input are considered in turn. These input scenarios have been chosen so as to provide an intuitive understanding of the dynamics of the Hodgkin–Huxley model.

The most important property of the Hodgkin–Huxley model is its ability to generate action potentials. In Fig. 2.6a an action potential has been initiated by a short current pulse of 1 ms duration applied at $t = 1$ ms. The spike has an amplitude of nearly 100 mV and a width at half maximum of about 2.5 ms. After the spike, the membrane potential falls below the resting potential and returns only slowly back to its resting value of -65 mV.

Ion channel dynamics during spike generation

In order to understand the biophysics underlying the generation of an action potential we return to Fig. 2.3a. We find that m_0 and n_0 increase with u whereas h_0 decreases. Thus, if some external input causes the membrane voltage to rise, the conductance of sodium channels increases due to increasing m. As a result, positive sodium ions flow into the cell and raise the membrane potential even further. If this positive feedback is large enough, an action potential is initiated. The explosive increase comes to a natural halt when the membrane potential approaches the reversal potential E_{Na} of the sodium current.

https://doi.org/10.1017/CBO9781107447615.003 Published online by Cambridge University Press

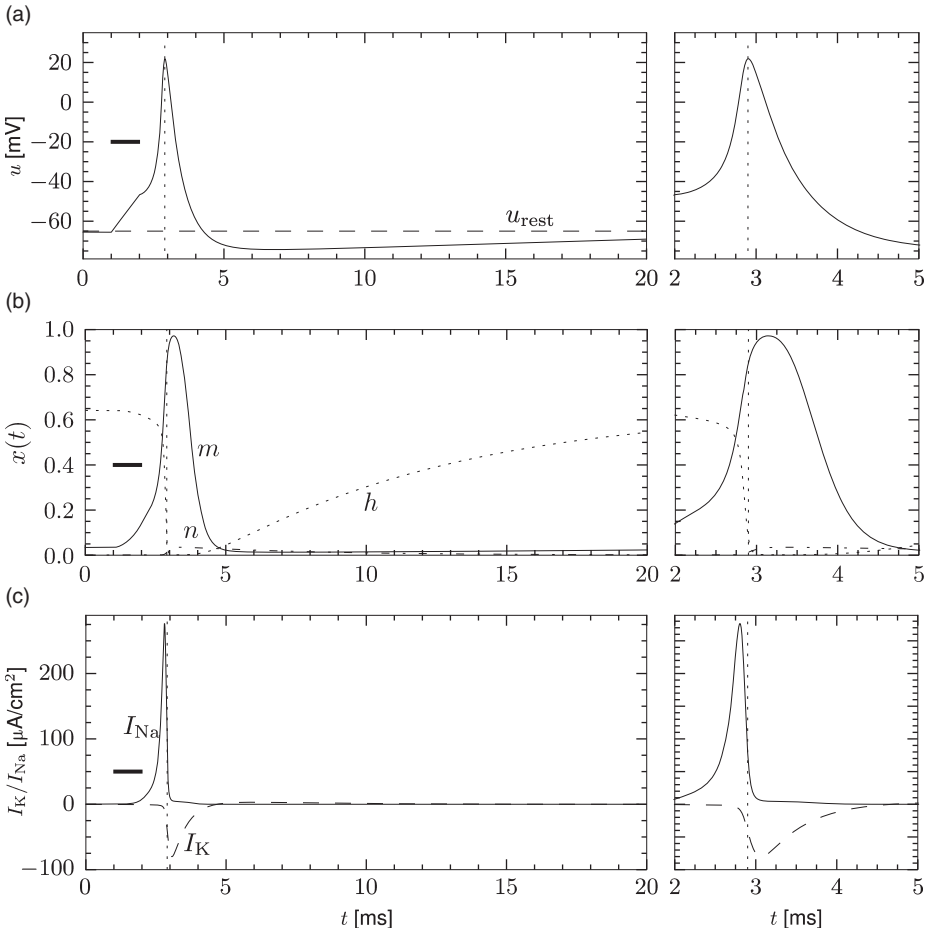

Fig. 2.6 (a) Action potential. The Hodgkin–Huxley model is stimulated by a short, but strong, current pulse between $t = 1$ ms and $t = 2$ ms. The time course of the membrane potential $u(t)$ for $t > 2$ ms shows the action potential (positive peak) followed by a relative refractory period where the potential is below the resting potential $u_{\rm rest}$ (dashed line). The right panel shows an expanded view of the action potential between $t = 2$ ms and $t = 5$ ms. (b) The dynamics of gating variables m, h, n illustrate how the action potential is mediated by sodium and potassium channels. (c) The sodium current $I_{\rm Na}$ which depends on the variables m and h has a sharp peak during the upswing of an action potential. The potassium current $I_{\rm K}$ is controlled by the variable n and starts with a delay compared with $I_{\rm Na}$.

At high values of u the sodium conductance is slowly shut off due to the factor h. As indicated in Fig. 2.3b, the "time constant" τ_h is always larger than τ_m. Thus the variable h which inactivates the channels reacts more slowly to the voltage increase than the variable m which opens the channel. On a similar slow time scale, the potassium (K^+) current sets in Fig. 2.6c. Since it is a current in outward direction, it lowers the potential. The overall effect of the sodium and potassium currents is a short action potential followed by

https://doi.org/10.1017/CBO9781107447615.003 Published online by Cambridge University Press

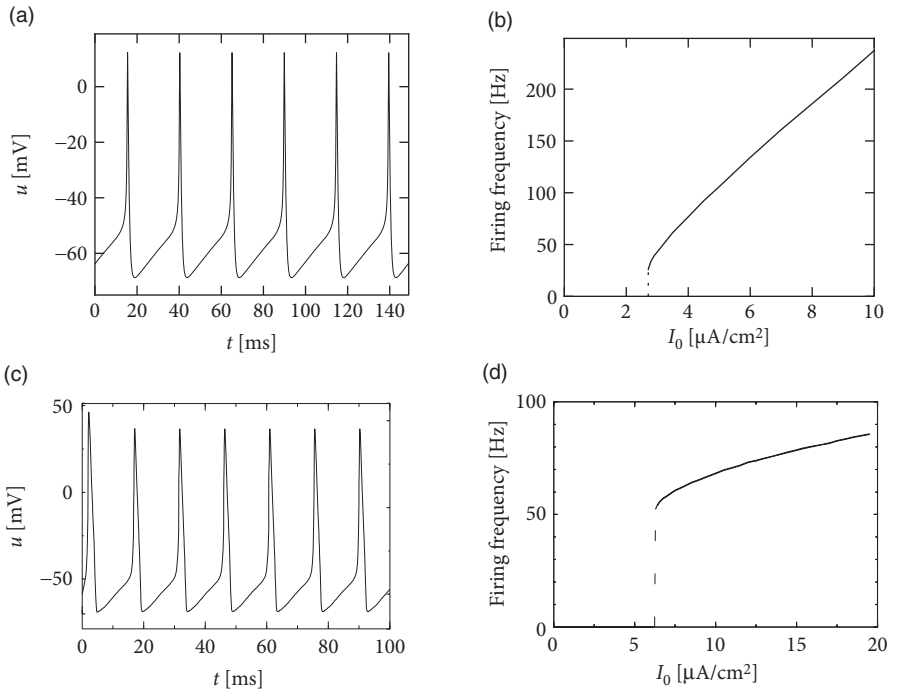

Fig. 2.7 (a) Spike train of the Hodgkin–Huxley model (with the parameters used in this book) for constant input current I_0. (b) Gain function. The mean firing rate ν is plotted as a function of I_0. The gain function of the Hodgkin–Huxley model is of type II, because it exhibits a jump. (c) Same as (a), but for the original parameters found by Hodgkin and Huxley to describe the ion currents in the giant axon of the squid. (d) Gain function for the model in (c).

a negative overshoot; see Fig. 2.6a. The negative overshoot, called hyperpolarizing spike-afterpotential, is due to the slow de-inactivation of the sodium channel, caused by the h-variable.

Example: Mean firing rates and gain function

The Hodgkin–Huxley equations (2.4)–(2.9) may also be studied for constant input $I(t) = I_0$ for $t > 0$. (The input is zero for $t \leq 0$.) If the value I_0 is larger than a critical value $I_\theta \approx 2.7\,\mu\text{A/cm}^2$, we observe regular spiking; see Fig. 2.7a. We may define a firing rate $\nu = 1/T$ where T is the interspike interval.

The firing rate as a function of the constant input I_0, often called the "frequency–current" relation or "f–I plot," defines the gain function plotted in Fig. 2.7b. With the parameters given in Table 2.1, the gain function exhibits a jump at I_θ. Gain functions with a discontinuity are called "type II."

https://doi.org/10.1017/CBO9781107447615.003 Published online by Cambridge University Press

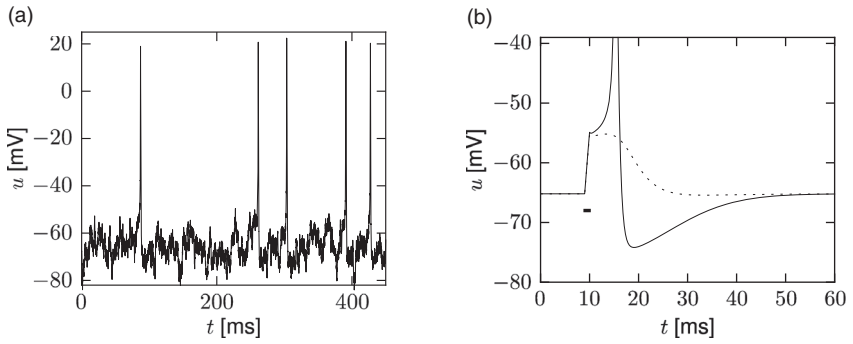

Fig. 2.8 (a) Spike train of the Hodgkin–Huxley model driven by a time-dependent input current. The action potentials occur irregularly. The figure shows the voltage u as a function of time. (b) Threshold effect. A short current pulse of 1 ms is applied which leads to a excursion of the membrane potential of a few millivolts (dashed line). A slight increase of the strength of the current pulse leads to the generation of an action potential (solid line) with an amplitude of about 100 mV above rest (out of bounds).

If we shift the curve of the inactivation variable h to more positive voltages, and keep the same parameters otherwise, the modified Hodgkin–Huxley model exhibits a smooth gain function; see Section 2.3.2 and Fig. 2.11. Neuron models or, more generally, "excitable membranes" are called "type I" or "class I" if they have a continuous frequency–current relation. The distinction between the excitability of type I and II can be traced back to Hodgkin (1948).

Example: Stimulation by time-dependent input

In order to explore a more realistic input scenario, we stimulate the Hodgkin–Huxley model by a time-dependent input current $I(t)$ that is generated by the following procedure. Every 2 ms, a random number is drawn from a Gaussian distribution with zero mean and standard deviation $\sigma = 34$ μA/cm^2. To get a continuous input current, a linear interpolation was used between the target values. The resulting time-dependent input current was then applied to the Hodgkin–Huxley model (2.4)–(2.6). The response to the current is the voltage trace shown in Fig. 2.8a. Note that action potentials occur at irregular intervals.

Example: Firing threshold

In Fig. 2.8b an action potential (solid line) has been initiated by a short current pulse of 1 ms duration. If the amplitude of the stimulating current pulse is reduced below some

https://doi.org/10.1017/CBO9781107447615.003 Published online by Cambridge University Press

critical value, the membrane potential (dashed line) returns to the rest value without a large spike-like excursion; see Fig. 2.8b. Thus we have a threshold-type behavior.

If we increased the amplitude of the current by a factor of 2, but reduced the duration of the current pulse to 0.5 ms, so that the current pulse delivers exactly the same electric charge as before, the response curves in Fig. 2.8b would look exactly the same. Thus, the threshold of spike initiation can *not* be defined via the amplitude of the current pulse. Rather, it is the charge delivered by the pulse or, equivalently, the membrane voltage immediately after the pulse, which determines whether an action potential is triggered or not. However, while the notion of a voltage threshold for firing is useful for a qualitative understanding of spike initiation in response to current pulses, it is in itself not sufficient to capture the dynamics of the Hodgkin–Huxley model; see the discussion in this and the next two chapters.

Example: Refractoriness

In order to study neuronal refractoriness, we stimulate the Hodgkin–Huxley model by a first current pulse that is sufficiently strong to excite a spike. A second current pulse of the *same* amplitude as the first one is used to probe the responsiveness of the neuron during the phase of hyperpolarization that follows the action potential. If the second stimulus is not sufficient to trigger another action potential, we have a clear signature of neuronal refractoriness. In the simulation shown in Fig. 2.9, a second spike is not emitted if the second stimulus is given less than 40 ms after the first one. It would, of course, be possible to trigger a second spike after a shorter interval, if a significantly stronger stimulation pulse was used; for classical experiments along those lines (see, e.g., Fuortes and Mantegazzini 1962).

If we look more closely at the voltage trajectory of Fig. 2.9, we see that neuronal refractoriness manifests itself in two different forms. First, owing to the hyperpolarizing spike-afterpotential, the voltage is lower. More stimulation is therefore needed to reach the firing threshold. Second, since a large portion of channels are open immediately after a spike, the resistance of the membrane is reduced compared with the situation at rest. The depolarizing effect of a stimulating current pulse therefore decays faster immediately after the spike than 10 ms later. An efficient description of refractoriness plays a major role in simplified neuron models discussed in Chapter 6.

Example: Damped oscillations and transient spiking

When stimulated with a small step-increase in current, the Hodgkin–Huxley model with parameters as in Table 2.1 exhibits a damped oscillation with a maximum of about

https://doi.org/10.1017/CBO9781107447615.003 Published online by Cambridge University Press

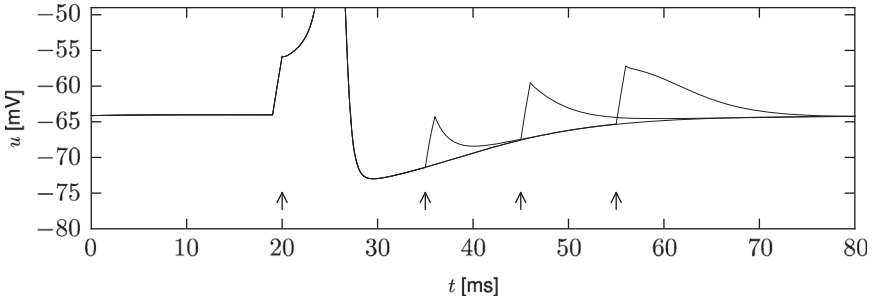

Fig. 2.9 Refractoriness of the Hodgkin–Huxley model. At $t = 20$ ms the model is stimulated by a short current pulse (left arrow) so as to trigger an action potential. A second current pulse of the same amplitude applied at $t = 35, 45$, or 55 ms (subsequent arrows) is not sufficient to trigger a second action potential.

20 ms after the onset of the current step; see Fig. 2.10. If the step size is large enough, but not sufficient to cause sustained firing, a single spike can be generated. Note that in Fig. 2.10 the input current returns at 200 ms to the *same* value it had a hundred milliseconds before. While the neuron stays quiescent after the first step, it fires a transient spike the second time not because the total input is stronger but because the step *starts* from a strong negative value.

A spike which is elicited by a step current that starts from a strong negative value and then switches back to zero would be called a rebound spike. In other words, a rebound spike is triggered by release from inhibition. For example, the Hodgkin–Huxley model with the original parameters for the giant axon of the squid exhibits rebound spikes when a prolonged negative input current is stopped; the model with the set of parameters adopted in this book, however, does not.

The transient spike in Fig. 2.10 occurs about 20 ms after the start of the step. A simple explanation of the transient spike is that the peak of the membrane potential oscillation after the step reaches the voltage threshold for spike initiation, so that a single action potential is triggered. It is indeed the subthreshold oscillations that underly the transient spiking illustrated in Fig. 2.10.

Damped oscillations result from subthreshold inactivation of the sodium current. At rest the sodium currents are not activated ($m \approx 0$) but only partially inactivated ($h \approx 0.6$). Responding to the step stimulus, the membrane potential increases, which activates slightly and de-inactivates slowly the sodium channel. When the input is not strong enough for an action potential to be initiated, the de-inactivation of I_{Na} reduces the effective drive and thus the membrane potential. The system then relaxes to an equilibrium. If, on the other hand, the current was strong enough to elicit a spike, the equilibrium may be reached only after the spike. A further increase in the step current drives sustained firing (Fig. 2.10).

https://doi.org/10.1017/CBO9781107447615.003 Published online by Cambridge University Press

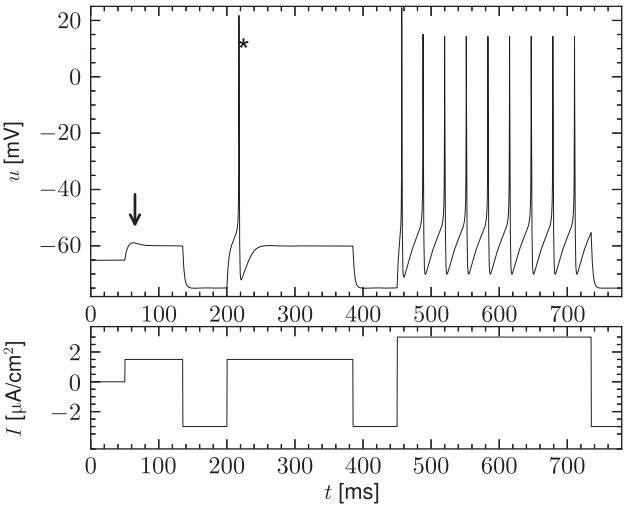

Fig. 2.10 Damped oscillations and a transient spike. Top. The voltage response to a step current shows a damped oscillation (arrow), a single rebound spike (asterisk) or repetitive firing. Bottom. Time course of the stimulating current.

2.3 The zoo of ion channels

Hodgkin and Huxley used their equations to describe the electrophysiological properties of the giant axon of the squid. These equations capture the essence of spike generation by sodium and potassium ion channels. The basic mechanism of generating action potentials is a short influx of sodium ions that is followed by an efflux of potassium ions. This mechanism of spike generation is essentially preserved in higher organisms, so that, with the choice of parameters given in Table 2.1, we already have a first approximate model of neurons in vertebrates. With a further change of parameters we could adapt the model equations to different temperatures to account for the fact that neurons at 37 degrees Celsius behave differently than neurons in a lab preparation held at a room temperature of 21 degrees Celsius.

However, in order to account for the rich biophysics observed in the neurons of the vertebrate nervous system, two types of ion channel are not enough. Neurons come in different types and exhibit different electrical properties which in turn correspond to a large variety of ion channels. Today, about 200 ion channels are known and many of these have been identified genetically (Ranjan *et al.*, 2011). In experimental laboratories where the biophysics and functional role of ion channels are investigated, specific ion channel types can be blocked through pharmacological manipulations. In order to make predictions of blocking results, it is important to develop models that incorporate multiple ion channels. As we shall see below (Section 2.3.1), the mathematical framework of the Hodgkin–Huxley model is well suited for such an endeavor.

For other scientific questions, we may be interested only in the firing pattern of neurons and not in the biophysical mechanisms that give rise to it. Later, in Part II of this book,

https://doi.org/10.1017/CBO9781107447615.003 Published online by Cambridge University Press

we will show that generalized integrate-and-fire models can account for a large variety of neuronal firing patterns (Chapter 6) and predict spike timings of real neurons with high precision (Chapter 11). Therefore, in Parts III and IV of the book, where we focus on large networks of neurons, we mainly work with generalized integrate-and-fire rather than biophysical models. Nevertheless, biophysical models, i.e., Hodgkin–Huxley equations with multiple ion channels, serve as an important reference.

2.3.1 Framework for biophysical neuron models

The formalism of the Hodgkin–Huxley equation is extremely powerful, because it enables researchers to incorporate known ion channel types into a given neuron model. Just as before, the electrical properties of a patch of neuronal membrane are described by the conservation of current

$$C\frac{\mathrm{d}u}{\mathrm{d}t} = -\sum_k I_k(t) + I(t)\,, \tag{2.10}$$

but in contrast to the simple Hodgkin–Huxley model discussed in the previous section, the right-hand side now contains all types of ion current found in a given neuron. For each ion channel type k, we introduce activation and inactivation variables

$$I_k(t) = g_k([Ca^{++}], \ldots) m^{p_k} h^{q_k} (u - E_k), \tag{2.11}$$

where m and h describe activation and inactivation of the channel with equations analogous to (2.6), p_k and q_k are empirical parameters, E_k is the reversal potential, and g_k is the maximum conductance which may depend on secondary variables such as the concentration of calcium, magnesium, dopamine or other substances. In principle, if the dynamics of each channel type (i.e., all parameters that go into Eqs. (2.11) and (2.6)) are available, then one needs only to know which channels are present in a given neuron in order to build a biophysical neuron model. Studying the composition of messenger RNA in a drop of liquid extracted from a neuron gives a strong indication of which ion channels are present in a neuron, and which are not (Toledo-Rodriguez *et al*., 2004). The relative importance of ion channels is not fixed, but depends on the age of neuron as well as other factors. Indeed, a neuron can tune its spiking dynamics by regulating its ion channel composition via a modification of the gene expression profile.

Ion channels are complex transmembrane proteins which exist in many different forms. It is possible to classify an ion channel using (i) its genetic sequence; (ii) the ion type (sodium, potassium, calcium, ...) that can pass through the open channel; (iii) its voltage dependence; (iv) its sensitivity to second-messengers such as intracellular calcium; (v) its presumed functional role; (vi) its response to pharmacological drugs or to neuromodulators such as acetylcholine and dopamine.

Using a notation that mixes the classification schemes (i)–(iii), geneticists have distinguished multiple families of voltage-gated ion channels on the basis of similarities in

https://doi.org/10.1017/CBO9781107447615.003 Published online by Cambridge University Press

the amino acid sequences. The channels are labeled with the chemical symbol of the ion of their selectivity, one or two letters denoting a distinct characteristic and a number to determine the subfamily. For instance "Kv5" is the fifth subfamily of the voltage-sensitive potassium channel family "Kv". An additional number may be inserted to indicate the channel isoforms, for instance "Nav1.1" is the first isoform that was found within the first subfamily of voltage-dependent sodium channels. Sometimes a lower-case letter is used to point to the splice variants (e.g., "Nav1.1a"). Strictly speaking, these names apply to a single cloned gene which corresponds to a channel subunit, whereas the full ion channel is composed of several subunits usually from a given family but possibly from different subfamilies.

Traditionally, electrophysiologists have identified channels with subscripts that reflect a combination of the classification schemes (ii)–(vi). The index of the potassium "M-current" I_M points to its response to pharmacological stimulation of Muscarinic (M) acetylcholine receptors. Another potassium current, I_{AHP}, shapes the after-hyperpolarization (AHP) of the membrane potential after a spike. Thus the subscript corresponds to the presumed functional role of the channel. Sometimes the functionally characterized current can be related to the genetic classification; for instance I_{AHP} is a calcium-dependent potassium channel associated with the small-conductance "SK" family, but in other cases the link between an electrophysiologically characterized channel and its composition in terms of genetically identified subunits is still uncertain. Linking genetic expression with a functionally characterized ion current is a fast-expanding field of study (Ranjan *et al.*, 2011).

In this section we select a few examples from the zoo of ion channels and illustrate how ion channels can modify the spiking dynamics. The aim is not to quantitatively specify parameters of each ionic current as this depends heavily on the genetic expression of the subunits, cell type, temperature and neurotransmitters. Rather, we would like to explore qualitatively the influence of ion channel kinetics on neuronal properties. In other words, let us bring the zoo of ion channels to the circus and explore the stunning acts that can be achieved.

2.3.2 Sodium ion channels and the type-I regime

The parameters of the Hodgkin–Huxley model in Table 2.1 relate to only one type of sodium and potassium ion channel. There are more than 10 different types of sodium channels, each with a slightly different activation and inactivation profile. However, as we shall see, even a small change in the ion channel kinetics can profoundly affect the spiking characteristics of a neuron.

Let us consider a sodium ion channel which has its inactivation curve $h_0(u)$ (Fig. 2.3a) shifted to depolarized voltages by 20 mV compared with the parameters in Table 2.1. With maximal conductances $g_{\mathrm{Na}} = 25\,\mathrm{nS/cm^2}$ and $g_{\mathrm{K}} = 40\,\mathrm{nS/cm^2}$, the dynamics of a neuron with this modified sodium channel (Fig. 2.11) is qualitatively different from that of a neuron with the parameters as in Table 2.1 (Figs. 2.7 and 2.10).

https://doi.org/10.1017/CBO9781107447615.003 Published online by Cambridge University Press

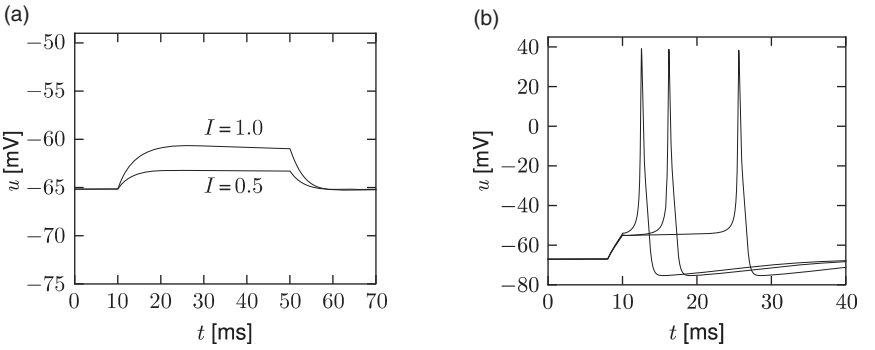

Fig. 2.11 A modification of sodium channel kinetics leads to different neuronal dynamics. (a) Response of a model with modified sodium channel to current steps of different amplitudes. (b) Delayed spike initiation. A short current pulse of 2 ms duration is applied at $t = 8$ ms. The action potential that is elicited in response to the current pulse is shown for decreasing pulse amplitudes ($I = 6.25, 5.90, 5.88\,\mu\text{A/cm}^2$). Note that the action potential can occur more than 10 ms *after* the end of the current pulse.

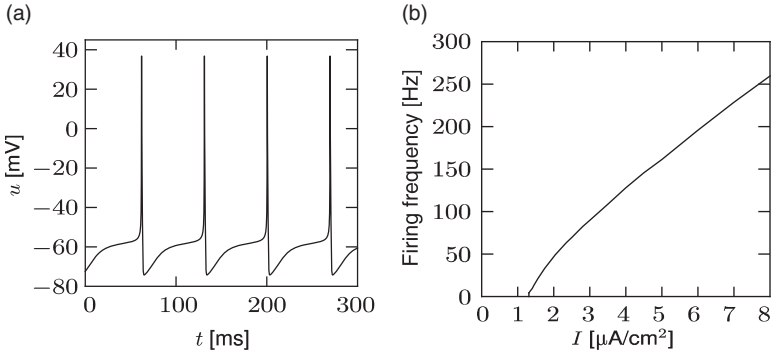

Fig. 2.12 Type-I regime with a modified sodium current. (a) Regular spiking response to constant input. (b) Firing frequency as a function of the constant current.

First, the neuron with the modified sodium dynamics shows no damped oscillations in response to a step input (Fig. 2.11a). Second, the neuron responds to a short current pulse which is just slightly above the firing threshold with a delayed action potential (Fig. 2.11b). Third, during regular spiking the shape of the action potential is slightly different in the model with the modified sodium channel (Fig. 2.12a). In particular, the membrane potential between the spikes exhibits an inflection point, unlike the spike train with the original set of parameters (Fig. 2.7a). Finally, the gain function (frequency–current plot) has no gap so that the neuron model can fire at arbitrarily small frequencies (Fig. 2.12b). If we compare this f–I plot with the gain function of the neuron with parameters from Table

2.1, we can distinguish two types of excitability: type I has a continuous input–output function (Fig. 2.12b), while type II has a discontinuity (Fig. 2.7b).

2.3.3 Adaptation and refractoriness

We have seen in Section 2.2 that the combination of sodium and potassium channels generates spikes followed by a relative refractory period. The refractoriness is caused by the slow return of the sodium inactivation variable h and the potassium activation variable n to their equilibrium values. The time scale of recovery in the Hodgkin–Huxley model, with parameters as in Table 2.1, is 4 ms for the potassium channel activation and 20 ms for the sodium channel inactivation. Other ion channel types, not present in the original Hodgkin–Huxley model, can affect the recovery process on much longer time scales and lead to spike-frequency adaptation: after stimulation with a step current, interspike intervals get successively longer. The basic mechanism of adaptation is the same as that of refractoriness: either a hyperpolarizing current is activated during a spike (and slowly de-activates thereafter) or a depolarizing current is inactivated during a spike and de-inactivates on a much slower time scale.

Example: Slow inactivation of a hyperpolarizing current

Let us start with the muscarinic potassium channel I_M, often called M-current. Genetically, the channel is composed of subunits of the Kv7 family. Figure 2.13a,b show the activation function as well as the voltage dependence of the time constant as characterized by Yamada *et al.* (1989). The activation function (Fig. 2.13a) tells us that this channel tends to be activated at voltages above 40 mV and is de-activated below 40 mV with a very sharp transition between the two regimes. Since 40 mV is well above the threshold of spike initiation, the membrane potential is never found above 40 mV except during the 1–2 ms of a spike. Therefore the channel partially activates during a spike and, after the end of the action potential, de-activates with a time constant of 40–60 ms (Fig. 2.13b). The slow deactivation of this potassium channel affects the time course of the membrane potential after a spike. Compared with the original Hodgkin–Huxley model, which has only the two currents specified in Table 2.1, a model with an additional I_M current exhibits a prolonged hyperpolarizing spike-afterpotential and therefore a longer relative refractory period (Fig. 2.13c–e).

In the regular firing regime, it is possible that the M-current caused by a previous spike is still partially activated when the next spike is emitted. The partial activation can therefore accumulate over successive spikes. By cumulating over spikes, the activation of I_M gradually forces the membrane potential away from the threshold, increasing the interspike interval. This results in a spiking response that appears to "adapt" to a step input, hence the name "spike-frequency adaptation" or simply "adaptation" (Fig. 2.13c–e).

https://doi.org/10.1017/CBO9781107447615.003 Published online by Cambridge University Press

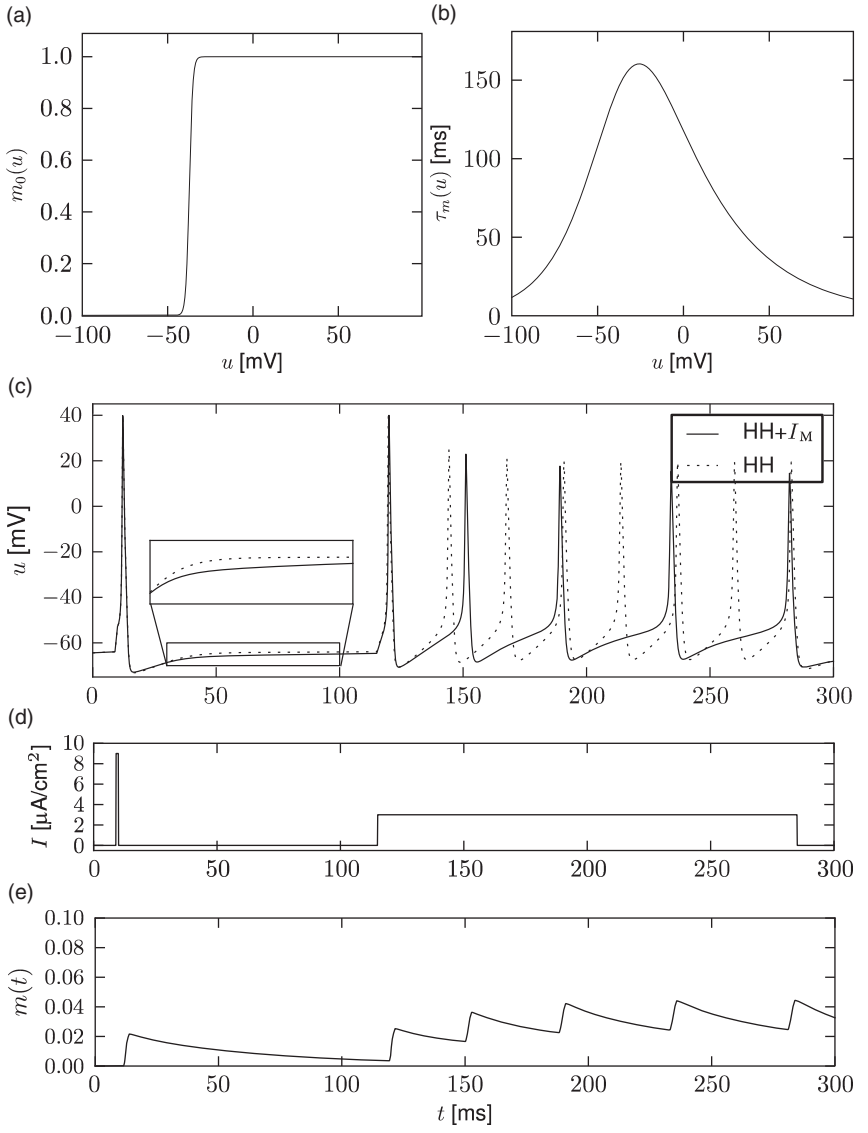

Fig. 2.13 Spike-frequency adaptation with I_M. (a) Voltage dependence of the stationary value of the activation variable m and (b) its time constants for the muscarinic potassium current $I_M = g_M m(u - E_k)$ extracted from experimental observations (Yamada *et al.*, 1989). (c) Voltage response to the current shown in (d) of the original Hodgkin–Huxley model with parameters from Table 2.1 (dashed line) and a model which also contains the I_M channel. The model with I_M exhibits adaptation. (e) Progressive activation of the potassium current I_M during the repetitive spiking period shown in (c).

https://doi.org/10.1017/CBO9781107447615.003 Published online by Cambridge University Press

Example: A-current

Another potassium ion channel with kinetics similar to I_M is I_A, but qualitatively different effects: I_A makes the relative refractory period longer and stronger without causing much adaptation. To see the distinction between I_A and I_M, we compare the activation kinetics of both channels (Figs. 2.13b and 2.14b). The time constant τ_m of activation is much faster for I_A than for I_M. This implies that the A-current increases rapidly during the short time of the spike and decays quickly afterward. In other words, the effect of I_A is short and strong whereas the effect of I_M is long and small. Because the effect of I_A does not last as long, it contributes to refractoriness, but only very little to spike frequency adaptation (Fig. 2.14c–e). Even though an inactivation process, with variable h, was reported for I_A, its time constant τ_h is so long (>150 ms) that it does not play a role in the above arguments.

Example: Slow extrusion of calcium

Multiple ion channel families contribute to spike-frequency adaptation. In contrast to the direct action of I_M, the calcium-dependent potassium channel $I_{\mathrm{K[Ca]}}$ generates adaptation indirectly via its dependence on the intracellular calcium concentration. During each spike, calcium enters through the high-threshold calcium channel I_{HVA}. As calcium accumulates inside the cell, the calcium-dependent potassium channel $I_{\mathrm{K[Ca]}}$ gradually opens, lowers the membrane potential, and makes further spike generation more difficult. Thus, the level of adaptation can be read out from the intracellular calcium concentration.

In order to understand the accumulation of calcium, we need to discuss the high-threshold calcium channel I_{HVA}. Since it activates above $-40\,\mathrm{mV}$ to $-30\,\mathrm{mV}$, the channel opens during a spike. Its dynamics is therefore similar to that of the sodium current, but the direct effect of I_{HVA} on the shape of the spike is small. Its main role is to deliver a pulse of calcium ions into the neuron. The calcium ions have an important role as second-messengers; they can trigger various cascades of biophysical processes. Intracellular calcium is taken up by internal buffers, or slowly pumped out of the cell, leading to an intricate dynamics dependent on the properties of calcium buffers and calcium pumps. For small calcium transients, however, or when the calcium pump has high calcium affinity and slow extrusion rate, the intracellular calcium dynamics follow (Helmchen *et al*., 2011)

$$\frac{\mathrm{d}[\mathrm{Ca}]}{\mathrm{d}t} = \phi_{\mathrm{Ca}} I_{\mathrm{Ca}} + \tau_{\mathrm{Ca}}^{-1} \left([\mathrm{Ca}] - [\mathrm{Ca}]_0\right), \tag{2.12}$$

where [Ca] denotes the intracellular calcium concentration, I_{Ca} is the sum of currents coming from all calcium ion channels, ϕ_{Ca} is a constant that scales the ionic current to changes in ionic concentration, $[\mathrm{Ca}]_0$ is a baseline intracellular calcium concentration,

https://doi.org/10.1017/CBO9781107447615.003 Published online by Cambridge University Press

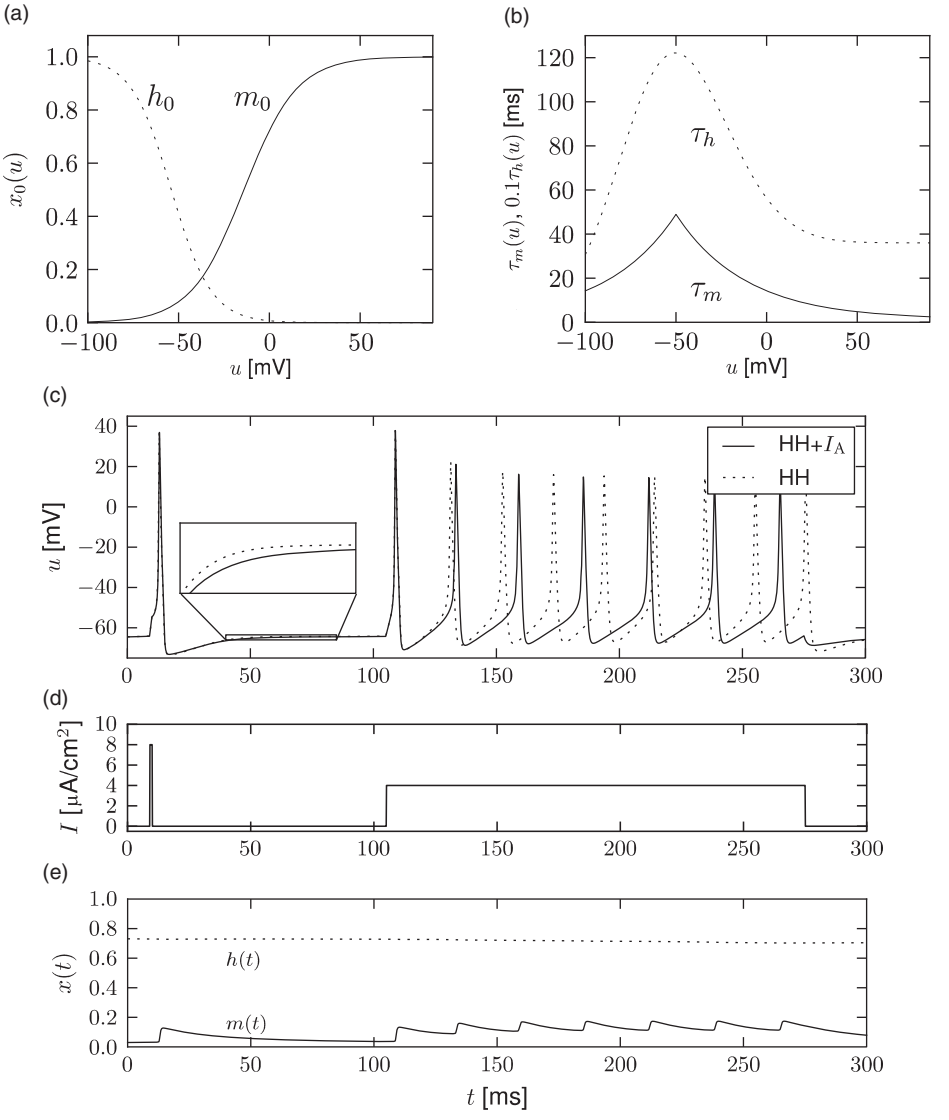

Fig. 2.14 I_A and the refractory period. (a) Voltage dependence of the stationary values and (b) time constants of the activation variable m and inactivation variable h for the A-type potassium current $I_A = g_A m h (u - E_K)$ extracted from experimental observations in pyramidal neurons of the cortex (Korngreen and Sakmann, 2000). (c) Voltage response to the current shown in (d), consisting of a single pulse and a step. (e) Progressive activation (solid line) and inactivation (dashed line) of the potassium current I_A during the stimulation shown in (c) and (d).

https://doi.org/10.1017/CBO9781107447615.003 Published online by Cambridge University Press

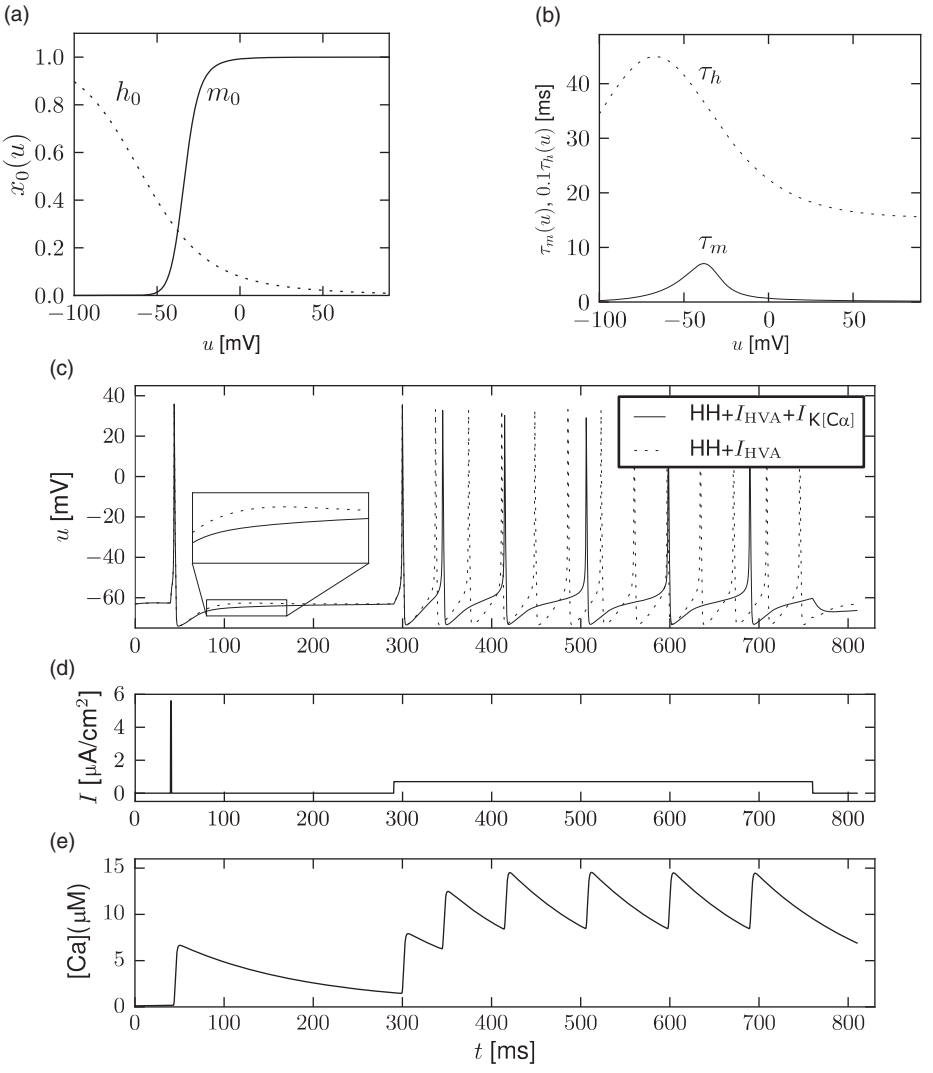

Fig. 2.15 Calcium-based spike-frequency adaptation with $I_{\mathrm{K[Ca]}}$ and I_{HVA}. (a) Voltage dependence of the stationary values. (b) Time constants of the activation variable m and inactivation variable h of the high-threshold calcium current $I_{\mathrm{HVA}} = g_{\mathrm{L}}\, h m (u - E_{\mathrm{Ca}})$ extracted from experiments (Reuveni *et al.*, 1993). (c) Voltage response of a Hodgkin–Huxley model with the calcium current I_{HVA} (dashed line) and a model that also contains a calcium-dependent potassium current $I_{\mathrm{K[Ca]}}$. (d) External current used for the simulation in (c) and (e). (e) Progressive accumulation of intracellular calcium in the two models.

https://doi.org/10.1017/CBO9781107447615.003 Published online by Cambridge University Press

and τ_{Ca} is the effective time constant of calcium extrusion. In our simple example the sole source of incoming calcium ions is the high-threshold calcium channel hence $I_{Ca} = I_{HVA}$. Because of the short duration of the spike, each spike adds a fixed amount of intracellular calcium which afterward decays exponentially (Fig. 2.15e), as observed in many cell types (Helmchen *et al.*, 2011).

The calcium-dependent potassium channel $I_{K[Ca]} = g_{K[Ca]}\, n\,(u - E_K)$ is weakly sensitive to the membrane potential but highly sensitive to intra cellular calcium concentration. The dynamics of activation can be modeled with a calcium-dependent time constant (Destexhe *et al.*, 1994a) of the activation variable n

$$\tau_n([\mathrm{Ca}]) = \frac{k_3}{1 + k_2 e^{k_1 [\mathrm{Ca}]}} \tag{2.13}$$

and a stationary value (Destexhe *et al.*, 1994a)

$$n_0 = \frac{k_2 e^{k_1 [\mathrm{Ca}]}}{1 + k_2 e^{k_1 [\mathrm{Ca}]}} \tag{2.14}$$

where k_1, k_2, k_3, and $g_{K[Ca]}$ are constants.

Figure 2.15 shows the effect of the combined action of calcium channel and $I_{K[Ca]}$. A single spike generates a transient increase in intracellular calcium which in turn causes a transient increase in $I_{K[Ca]}$ activation which results in a hyperpolarization of the membrane potential compared with a model without $I_{K[Ca]}$. During sustained stimulation, calcium accumulates over several spikes, so that the effect of $I_{K[Ca]}$ becomes successively larger and interspike intervals increase. The time constant associated with adaptation is a combination of the calcium extrusion time constant and the potassium activation and de-activation time constant.

Example: Slow de-inactivation of a persistent sodium channel

The stationary values of activation and inactivation of the persistent sodium channel I_{NaP} (Fig. 2.16a) are very similar to that of the normal sodium channel of the Hodgkin–Huxley model. The main difference lies in the time constant. While activation of the channel is quick, it inactivates on a much slower time scale. Hence the name: the current "persists". The time constant of the inactivation variable h is of the order of a second.

During sustained stimulation, each spike contributes to the inactivation of the sodium channel and therefore reduces the excitability of the neuron. This special type of refractoriness is not visible in the spike-afterpotential, but can be illustrated as a relative increase in the effective spiking threshold (Fig. 2.16b). Since, after a first spike, the sodium channel is partially inactivated, it becomes more difficult to make the neuron fire a second time.

https://doi.org/10.1017/CBO9781107447615.003 Published online by Cambridge University Press

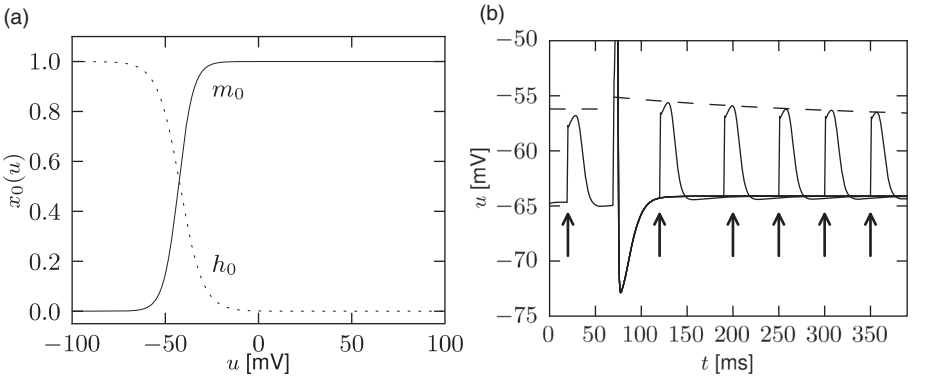

Fig. 2.16 The persistent sodium channel I_{NaP} increases the firing threshold. (a) Activation and inactivation profiles for $I_{\mathrm{NaP}} = g_{\mathrm{NaP}}\, m\, h\, (u - E_{\mathrm{Na}})$. Activation is fast (a few ms) whereas inactivation is of the order of a second as measured in pyramidal neurons of the cortex (Aracri *et al.*, 2006). (b) Slow inactivation affects the effective threshold. In a Hodgkin–Huxley model with persistent sodium current, subthreshold current pulses are injected at different moments (arrows). At $t = 75$ ms (asterisk) only, a suprathreshold stimulation was applied. Tuning the strength of the other current pulses so that they are just below spike initiation reveals an effective voltage threshold (dashed line) that is higher immediately after the first spike.

2.3.4 Subthreshold effects

Some ion channels have an activation profile $m_0(u)$ which has a significant slope well below the spike initiation threshold. During subthreshold activation of the cell by background activity *in vivo*, or during injection of a fluctuating current, these currents partially activate and inactivate, following the time course of membrane potential fluctuations and shaping them in turn.

We describe two examples of subthreshold ion channel dynamics. The first one illustrates adaptation to a depolarized membrane potential by inactivation of a depolarizing current, which results in a subsequent reduction of the membrane potential. The second example illustrates the opposite behavior: in response to a depolarized membrane potential, a depolarizing current is triggered which increases the membrane potential even further. The two examples therefore correspond to subthreshold adaptation and subthreshold facilitation, respectively.

Example: Subthreshold adaptation by I_h

Subthreshold adaptation through a hyperpolarization-activated current I_h is present in many cell classes. As the name implies, the current is activated only at hyperpolarized voltages as can be seen in Fig. 2.17a. Thus, the voltage dependence of the activation variable is inverted compared with the normal case and has *negative* slope. Therefore, the activation variable looks more like an inactivation variable and this is why we choose h as the symbol for the variable. The channel is essentially closed for prolonged membrane

https://doi.org/10.1017/CBO9781107447615.003 Published online by Cambridge University Press

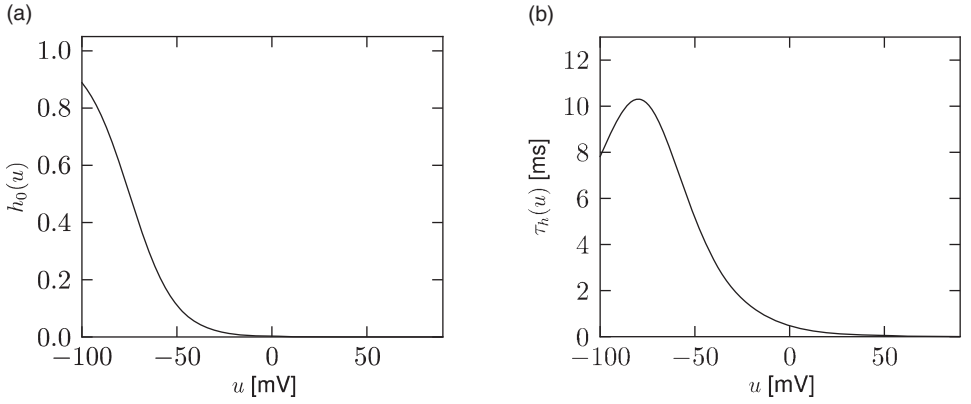

Fig. 2.17 Subthreshold adaptation with I_h. (a) Stationary values and (b) time constants of the variable h controlling the hyperpolarization-activated mixed current I_h as measured in pyramidal neurons of the hippocampus (Magee, 1998).

potential fluctuations above -30 mV. The I_h current is a non-specific cation current, meaning that sodium, potassium, and calcium can pass through the I_h channel when it is open. The reversal potential of this ion channel is usually around -45 mV so that the h-current $I_h = g_h\, h\,(u - E_h)$ is depolarizing at resting potential and over most of the subthreshold regime.

The presence of I_h causes the response to step changes in input current to exhibit damped oscillations. The interaction works as follows: suppose an external driving current depolarizes the cell. In the absence of ion channels this would lead to an exponential relaxation to a new value of the membrane potential of, say, -50 mV. Since I_h was mildly activated at rest, the membrane potential increase causes the channel to de-activate. The gradual closure of I_h removes the effective depolarizing drive and the membrane potential decreases, leading to a damped oscillation (as in Fig. 2.10). This principle can also lead to a rebound spike as seen in Fig. 2.10. Subthreshold adaptation and damped oscillations will be treated in more detail in Chapter 6.

Example: Subthreshold facilitation by I_{NaS}

The sodium ion channel I_{NaS} is slow to activate. Let us consider again stimulation with a step current using a model which contains both the fast sodium current of the Hodgkin–Huxley model and the slow sodium current I_{NaS}. If the strength of the current step is such that it does not activate the fast sodium channel but is strong enough to activate I_{NaS}, then the slow activation of this sodium current increases membrane potential gradually with the time constant of activation of the slow sodium current (Fig. 2.18b). The slow depolarization continues until the fast sodium current activates and an action potential

https://doi.org/10.1017/CBO9781107447615.003 Published online by Cambridge University Press

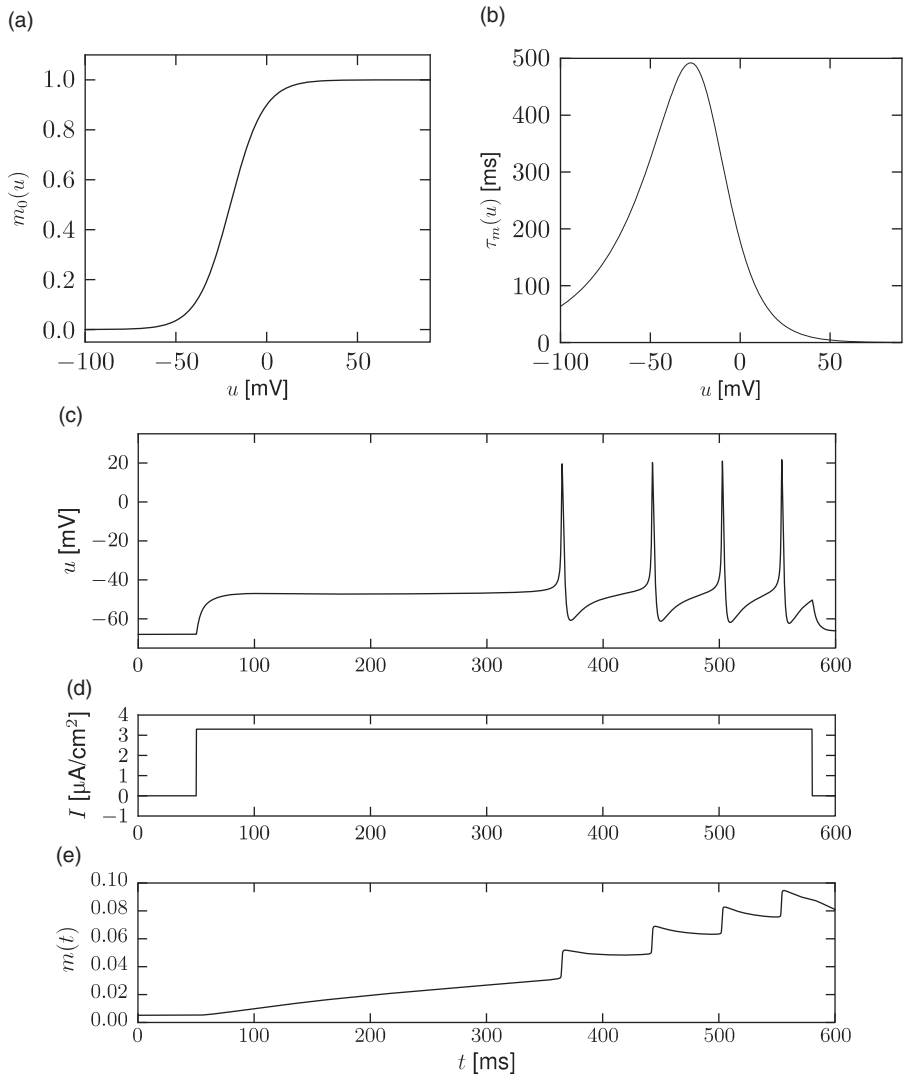

Fig. 2.18 Subthreshold facilitation with I_{NaS}. (a) Stationary values and (b) time constants of the activation variable m for the slow sodium current I_{NaS} similar to measurements done in pyramidal neurons of the hippocampus (Hoehn *et al*., 1993). (c) Voltage response. (d) External current. (e) Slow sodium current activation, leading to delayed spike initiation and firing frequency facilitation.

is generated (Fig. 2.18c). Such delayed spike initiation has been observed in various types of interneurons of the cortex. If the amplitude of the step current is sufficient to immediately activate the fast sodium channels, the gradual activation of I_{NaS} increases the firing frequency leading to spike-frequency facilitation.

https://doi.org/10.1017/CBO9781107447615.003 Published online by Cambridge University Press

2.3.5 Calcium spikes and postinhibitory rebound

Postinhibitory rebound means that a hyperpolarizing current which is suddenly switched off results in an overshoot of the membrane potential or even in the triggering of one or more action potentials. Through this mechanism, action potentials can be triggered by *inhibitory* input. These action potentials, however, occur with a certain delay after the arrival of the inhibitory input, i.e., after the end of the IPSP (Aizenman and Linden, 1999).

Inactivating currents with a voltage threshold below the resting potential, such as the low-threshold calcium current, can give rise to a much stronger effect of inhibitory rebound than the one seen in the standard Hodgkin–Huxley model. Compared with the sodium current, the low-threshold calcium current I_T has activation and inactivation curves that are shifted significantly toward a hyperpolarized membrane potential so that the channel is

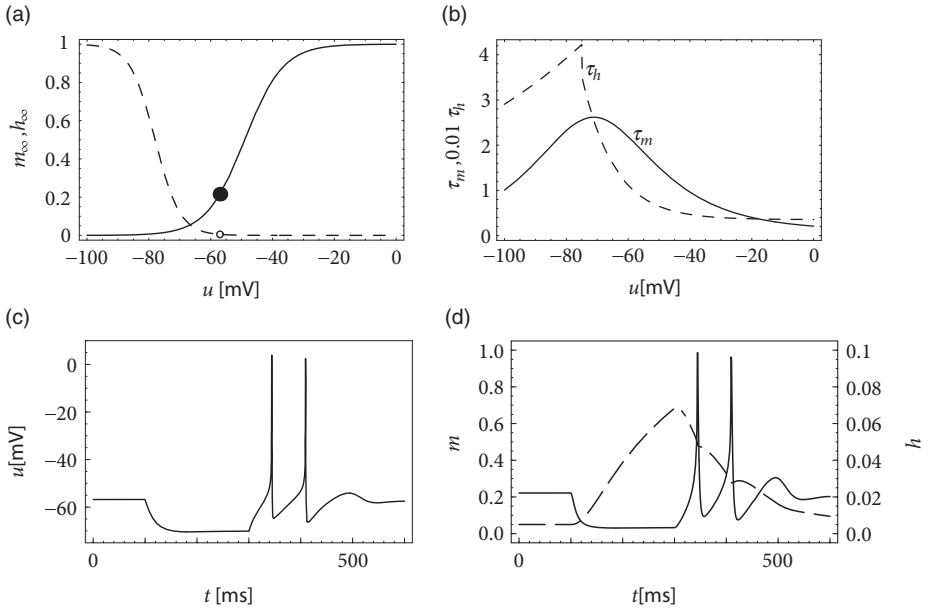

Fig. 2.19 Postinhibitory rebound through de-inactivation. (a) Activation $m_0(u)$ and inactivation $h_0(u)$ at equilibrium of the low-threshold calcium current I_T. Small circles indicate the equilibrium values of m and h at the resting potential. To de-inactivate the current, the membrane potential must be below rest. (b) The time constants of activation and inactivation. Note that different vertical scales have been used for τ_m and τ_h since the dynamics of the inactivation variable h is slower by a factor 10–100 than that of the activation variable m. Numerical values of parameters correspond to a model of neurons in the deep cerebellar nuclei (Kistler and van Hemmen, 2000). (c) Membrane potential as a function of time. Injection of a hyperpolarizing current pulse (100 pA during 200 ms from $t = 100$ ms to $t = 300$ ms) results, at the end of current injection, in a low-threshold calcium spike that in turn triggers two sodium action potentials. (d) Time course of activation (solid line, left scale) and inactivation (dashed line, right scale) variables of the I_T current that is responsible for this phenomenon.

https://doi.org/10.1017/CBO9781107447615.003 Published online by Cambridge University Press

completely *inactivated* ($h \approx 0$) at the resting potential; see Fig. 2.19a and b. In order to open the low-threshold calcium channels it is first of all necessary to remove its inactivation by *hyperpolarizing* the membrane. The time constant of the inactivation variable h is rather high and it thus takes a while until h has reached a value sufficiently above zero; see Fig. 2.19b and d. But even if the channels have been successfully "de-inactivated" they remain in a closed state, because the activation variable m is zero as long as the membrane is hyperpolarized. However, the channels will be transiently opened if the membrane potential is rapidly relaxed from the hyperpolarized level to the resting potential, because activation is faster than inactivation and, thus, there is a short period when both m and h are nonzero. The current that passes through the channels is terminated ("inactivated") as soon as the inactivation variable h has dropped to zero again, but this takes a while because of the relatively slow time scale of τ_h. The resulting current pulse is called a *low-threshold calcium spike* and is much broader than a sodium spike.

The increase in the membrane potential caused by the low-threshold calcium spike may be sufficient to trigger ordinary sodium action potentials. These are the rebound spikes that may occur after a prolonged inhibitory input. Figure 2.19c shows an example of (sodium) rebound spikes that ride on the broad depolarization wave of the calcium spike; note that the whole sequence is triggered at the end of an inhibitory current pulse. Thus release from inhibition causes here a spike-doublet.

2.4 Summary

The Hodgkin–Huxley model describes the generation of action potentials on the level of ion channels and ion current flow. It is the starting point for detailed biophysical neuron models which in general include more than the three types of currents considered by Hodgkin and Huxley. Electrophysiologists have described an overwhelming richness of different ion channels. The set of ion channels is different from one neuron to the next. The precise channel configuration in each individual neuron determines a good deal of its overall electrical properties.

Literature

A nice review of the Hodgkin–Huxley model including some historical remarks can be found in Nelson and Rinzel (1995). A comprehensive and readable introduction to the biophysics of single neurons is provided by the book of Christof (1999). Even more detailed information on ion channels and nonlinear effects of the nervous membrane can be found in B. Hille's book of *Ionic Channels of Excitable Membranes* (Hille, 2001). The rapidly growing knowledge of the genetic description of ion channel families and associated phenotypes is condensed in Channelpedia (Ranjan *et al*., 2011).

Exercises

1. **Nernst equation**. *Using the Nernst equation (Eq. 2.2) calculate the reversal potential of* Ca^{2+} *at room temperature (21 degrees Celsius), given an intracellular concentration of* 10^{-4} mM *and an extracellular concentration of* 1.5 mM.
2. **Reversal potential and stationary current–voltage relation**. *An experimenter studies an unknown ion channel by applying a constant voltage u while measuring the injected current I needed to balance the membrane current that passes through the ion channel.*

   (a) Sketch the current–voltage relationship (I as a function of u) assuming that the current follows $I_{\text{ion}} = g_{\text{ion}} m h\,(u - E_{\text{rev}})$ *with* $g_{\text{ion}} = 1$ nS *and* $E_{\text{rev}} = 0$ mV *where* $m = 0.1$ *and* $h = 1.0$ *are independent of the voltage.*

   (b) Sketch qualitatively the current–voltage relationship assuming that the current follows $I_{\text{ion}} = g_{\text{ion}} m h\,(u - E_{\text{rev}})$ *with* $g_{\text{ion}} = 1$ nS *and* $E_{\text{rev}} = 0$ mV *where* $m_0(u)$ *and* $h_0(u)$ *have the qualitative shape indicated in Fig. 2.15.*
3. **Activation time constant**. *An experimenter holds the channel from Fig. 2.15a and b at* $u = -50$ mV *for two seconds and then suddenly switches to* $u = 0$ mV. *Sketch the current passing through the ion channel as a function of time, assuming* $I_{\text{ion}} = g_{\text{ion}} m h\,(u - E_{\text{rev}})$ *with* $g_{\text{ion}} = 1$ nS *and* $E_{\text{rev}} = 0$ mV.
4. **The power of the exponent**. *An experimenter holds an unknown potassium ion channel with activation variable n with voltage dependence* $n_0(u)$ *and time constant* τ_n *at* $u = -50$ mV *for two seconds and then, at time* $t = 0$, *suddenly switches to* $u = 0$ mV.

   (a) Sketch the activation variable n, n^2, n^3 *as a function of time for times smaller than* τ_n.

   (b) Show mathematically that for $0 < t < \tau_n$ *the time course of the activation variable can be approximated* $n(t) = n_0(-50\text{mV}) + [n_0(0\text{mV}) - n_0(-50\text{mV})]t/\tau_m$.

   (c) Do you agree with the statement that "the exponent p in the current formula $I_{\text{ion}} = g_{\text{ion}} n^p\,(u - E_{\text{rev}})$ *determines the "delay" of activation"? Justify your answer.*
5. **Hodgkin–Huxley parameter estimation**. *Design a set of experiments to constrain all the parameters of the two ion channels of the Hodgkin–Huxley model. Assume that the neuron has only the* I_{Na} *and* I_{K} *currents and that you can use tetrodotoxin (TTX) to block the sodium ion channel and tetraethylammonium (TEA) to block the potassium ion channel.*

   Hint: Use the results of the previous exercises.
6. **Simplified expression of the activation function**. *Show that with the voltage-dependent parameters* $\alpha_m(u) = 1/[1 - e^{-(u+a)/b}]$ *and* $\beta_m(u) = 1/[1 - e^{-(u+a)/b}]$ *(compare Table 2.1), the stationary value of the activation variable can be written as* $m_0(u) = 0.5\,[1 + \tanh[\beta\,(u - \theta_{\text{act}})]]$. *Determine the activation threshold* θ_{act} *and the activation slope* β.

   Hint: $\tanh(x) = [\exp(x) - \exp(-x)]/[\exp(x) + \exp(-x)]$.

https://doi.org/10.1017/CBO9781107447615.003 Published online by Cambridge University Press